

Robust image transmission strategies for fading channels

Hervé BOEGLÉN, Olivier HAEBERLE
Laboratoire MIPS LABEL, IUT de Mulhouse
61 rue Albert Camus
68093 Mulhouse Cedex France
herve.boeglen@uha.fr

Christian CHATELLIER, Christian OLIVIER
Laboratoire SIC XLIM, UMR CNRS 6172
Téléport 2, Bd Marie et Pierre Curie
86962 Futuroscope Cedex France
chatellier@sic.sp2mi.univ-poitiers.fr

Abstract— The aim of this paper is to present a robust still-image transmission scheme and show its performance when used on a frequency flat fading channel. By following a Joint Source-Channel Coding approach, it is shown that image transmission with good visual quality is possible even with BER as high as 4%. Furthermore, this scheme only requires 26% redundancy for Error Control Coding (ECC). The ECC part can be completed by an original PDE-based restoration algorithm to further improve the visual quality of the image.

Keywords : Joint source-channel coding, image transmission, image compression, fading channels.

I. INTRODUCTION

The motivation of our work comes from the fact that the transmission of JPEG or JPEG2000 images over insecure noisy channels, even with low Bit Error Rates (BER), can lead to severe consequences on decoded visual information. The reason for such high error sensitivity is the adoption of Variable Length Coding (VLC) schemes. Although VLC are known to achieve better compression rates than Fixed-Length Codes (FLC), they also introduce dependence among codewords which is an obvious drawback in transmission applications. To answer this problem, the normalisation body in charge with JPEG2000 has created the JPEG Wireless (JPWL) extension. This extension allows protecting the sensitive parts of the JPEG2000 image (e.g. the headers) with different error correcting codes [1]. At full protection level, the code rate is 0.3 which means that 70% of the transmitted data is used for error correction. Other authors have proposed similar solutions where they use Reed-Solomon and Turbo codes to allow transmission of images on fading channels [2][3]. Their results show clearly the efficiency of their schemes but, again, the code rate used is in the order of 0.3.

From an information theory point of view, one can notice that these transmission schemes are typical illustrations of Shannon's separability theorem stating that source and channel coding can be designed efficiently separately. In fact, this theorem has also created two separate scientific communities namely the source coding and channel coding communities which have the point of view of their topics. However, Shannon's separability theorem does not say anything about complexity of such separately designed systems. This has led to another approach called Joint Source-Channel Coding

(JSCC) which aims at optimizing a transmission system while keeping its complexity as low as possible. The compressed image transmission scheme presented here has been designed by following this approach. This paper is organised as follows. Section II describes the Wavelet Transform Self-Organizing Map (WTSOM) image coding scheme considered throughout this paper. Section III is devoted to the strategies we have developed for the transmission of the WTSOM scheme over fading channels. In section IV we describe an original post-transmission Partial Differential Equations (PDE) based restoration algorithm. Finally results and concluding remarks are given in section V.

II. THE WTSOM IMAGE CODING SCHEME

The WTSOM image coding system combines two well-known techniques in the image processing community: Wavelet Transformation (WT) and Vector Quantization (VQ). The first step of our compression scheme consists in applying a wavelet decomposition up to level 3 using a Daubechies 9/7 filter bank to the original image. After this operation, we discard the less important subbands (in terms of visual rendering), keeping only the most significant ones (see Fig. 1).

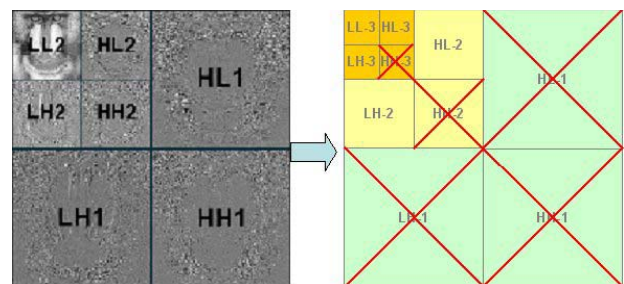


Figure 1. WTSOM Wavelet decomposition

The second step is to apply VQ on the remaining subbands of the wavelet decomposition. To do this, we use Kohonen's Self-Organizing Map (SOM) algorithm because of its interesting property of auto-organization: close vectors in terms of Euclidean distance correspond to close indices in terms of location in the self-organized codebook. The topological organisation of the codebooks is then used to define an optimized mapping of the quantized elements on a digital

modulation of appropriate size. This procedure ensures a very good resistance to transmission errors [4]. It is precisely this relation between the codebook organisation and the digital modulation symbols coding that defines our initial JSCC strategy. The corresponding transmission chain is represented in Fig. 2. Thanks to the above described techniques we obtain a compression rate in the order of 25 (0.3 bpp) for gray-scale images. The first WTSOM scheme used to transmit only gray-scale images so we decided to go a step further by applying the techniques presented previously on a color image. Taking into account works showing that human beings are more sensitive to fast luminosity changes than to fast color and saturation changes, we decided to adopt a $YCbCr$ color space rather than the traditional RGB color space. This representation has also the advantage of decorrelating the three color planes of the image. Finally, the preceding techniques are applied on the three color planes of the image except that in the case of the C_b and C_r planes we only keep the LL3 subbands. This yields a compression rate in the order of 42 (0.6 bpp).

The very good behavior of the system for BER values in the order of 2% over highly disturbed ionospheric channels [5] has led us to consider using the system over mobile fading channels. The main features of these channels and the ways to adapt the WTSOM scheme are described in the next section.

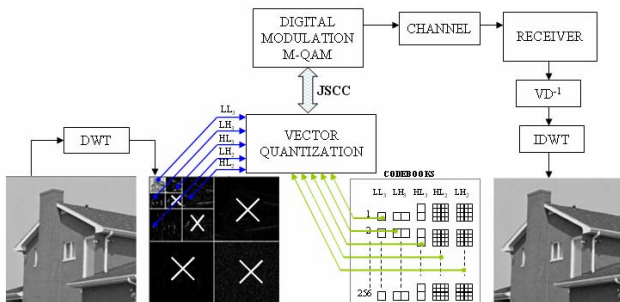


Figure 2. WTSOM transmission chain

III. TRANSMISSION STRATEGIES FOR FADING CHANNELS

A. Physical characteristics of fading channels

In mobile radio communications, the emitted electromagnetic waves often do not reach the receiving antenna directly due to obstacles blocking the line-of-sight (LOS) path. In fact, the receiving waves are a superposition of waves coming from all directions due to reflection, diffraction and scattering caused by buildings, trees and other obstacles. This effect is known as *multipath propagation* [6]. As a result, the received signal consists of an infinite sum of attenuated, delayed, and phase-shifted replicas of the transmitted signal, each influencing each other. Depending of the phase of each partial wave, the superposition can be constructive or destructive. Apart from that, when transmitting digital signals, the form of the transmitted impulse can be distorted during transmission and often several individually distinguishable impulses occur at the receiver due to multipath propagation. This effect is called *impulse dispersion*. The value of the impulse dispersion depends on the propagation delay

differences and the amplitude relations of the partial waves. The consequence of this effect is a distortion of the frequency response characteristic of the transmitted signal.

Besides the multipath propagation, also the *Doppler effect* [6] has a negative influence on the transmission characteristics of the mobile radio channel. Because of the mobility of the receiver, the Doppler effect causes a frequency shift of each of the partial waves. As a result, the spectrum of the transmitted signal undergoes a frequency expansion during transmission. This effect is called *frequency dispersion*. The value of the frequency dispersion mainly depends on the maximum Doppler frequency and the amplitudes of the received partial waves. In the time domain, the Doppler effect implicates that the Impulse Response (IR) of the channel becomes time-variant.

Multipath propagation in connection with the movement of the receiver and/or the transmitter leads to drastic and random fluctuations of the received signal. Fades of 30 to 40dB and more below the mean value of the received signal level can occur several times per second as can be seen in Fig. 3.

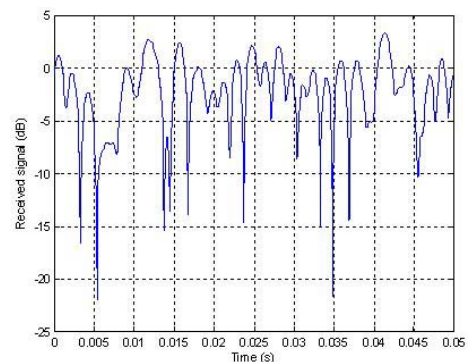


Figure 3. Fading channel received signal amplitude

In digital data transmission, the momentary fading of the received signal causes *burst errors* i.e. errors with strong connections with each others. Therefore, a fading interval produces burst errors, where the burst length is determined by the duration of the fading. Corresponding to this a connecting interval produces a bit sequence almost free of errors. From this, one can easily understand that developing efficient error protection strategies for digital transmission systems implicates a good knowledge of the fading channel statistics.

A mobile fading channel can be described by its Impulse Response (IR) which is made up of a large number of impulses coming from N_p different paths:

$$\underline{h}(\tau, t) = \sum_{p=1}^{N_p} a_p e^{j(2\pi f_{D,p} \tau + \phi_p)} \delta(\tau - \tau_p) \quad (1)$$

where a_p , $f_{D,p}$, ϕ_p et τ_p represent respectively the amplitude, the Doppler frequency, the phase and the propagation delay related to path p . It has been shown [6] that the channel can be described by a Wide-Sense Stationary (WSS) stochastic process where the different paths are uncorrelated (Uncorrelated Scattering or US). In this case, one can show [6] that the description of the IR $\underline{h}(t, \tau)$ correlation functions is

enough to characterise the channel's fading effect. Using these functions, one can have access to two important features of these channels namely the coherence bandwidth B_c and the coherence time T_c . The coherence bandwidth B_c is given by:

$$B_c \approx \frac{1}{5\sigma_\tau} \quad (2)$$

where σ_τ denotes the delay spread. B_c represents the bandwidth over which the frequency characteristics of the channel are correlated. The channel is said to be *frequency selective* if the signal bandwidth B is larger than B_c . The coherence time T_c of the channel is given by:

$$T_c \approx \frac{9}{16\pi f_{D_{\max}}} \quad (3)$$

where $f_{D_{\max}}$ denotes the maximal Doppler frequency. T_c corresponds to the duration when the channel is time invariant. The channel is said to be *time selective* if the symbol transmission time T_s is longer than T_c .

In order to evaluate the performance of our image transmission system we use a normalised WSSUS stochastic mobile fading channel of the COST207TU type [7].

B. Digital communication strategies for fading channels

Having in mind a low complexity system, we focus on situations where neither channel state information (CSI) nor reliable estimation of the carrier phase is available at the receiver side. In these situations, differential modulation/demodulation techniques have proved to be very robust due to the fact that they can mitigate the phase distortions caused by fading. Moreover, as no channel estimation is needed, the system complexity is reduced significantly. In order to keep the same bandwidth efficiency as in the AWGN case [5], we use a 16-point constellation that may be differentially encoded and decoded. This scheme is known as Star 16QAM or 16DAPSK [8] and uses a combination of independent 2DASK and 8DPSK. Three of the four bits are modulated by a Gray encoded 8DPSK. The remaining bit is amplitude modulated by a 2DASK scheme: a "0" doesn't change the amplitude while a "1" changes it. Fig. 4 shows the signal constellation of the 16DAPSK modulation. For our application we have optimised the 16DAPSK key parameters i.e. the ring ratio and the bit mapping. More details about this can be found in [9].

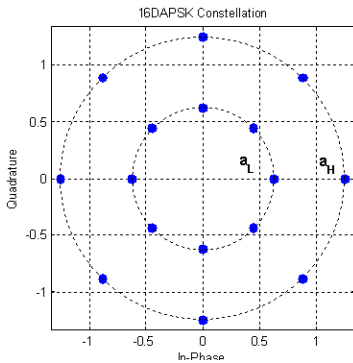


Figure 4. Star 16QAM constellation

Highly disturbed channels need appropriate forward error correction schemes. In order to keep our system bandwidth efficient, we have adopted high rate product codes which, on the one hand, allow keeping the image topological structure, and on the other hand, can be efficiently Turbo decoded.

Fig. 5 shows the structure of a product code. The encoding procedure is as follows. We start by filling a matrix of size $(k_1 \times k_2)$ with the data to be encoded. Then we encode the columns of length k_1 with code (n_1, k_1, d_1) . Finally, we encode the lines of length k_2 with the (n_2, k_2, d_2) . This yields a coded matrix of size $(n_1 \times n_2)$. One can show that the overall code rate is given by:

$$R = \frac{k_1}{n_1} \cdot \frac{k_2}{n_2} \quad (4)$$

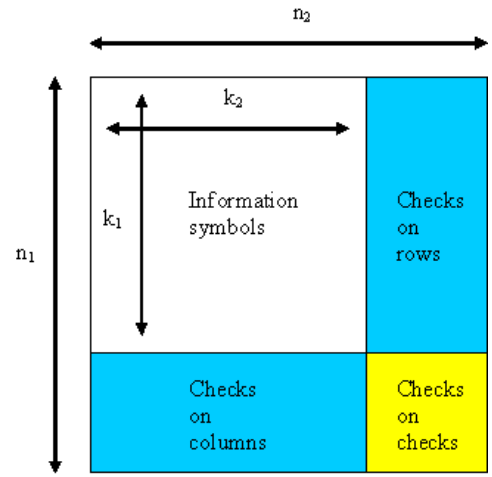


Figure 5. Product code construction

It is well known in the coding community that block codes perform better than convolutional codes when the coding rate $R > 0.6$. As we target our application for such rates, we have adopted simple Hamming codes as constituent codes for the product code. However, the main problem with block codes is that their classical decoding algorithms use algebraic methods yielding hard decoding. This is a loss of about 2dB compared to soft decoding, a significant amount we cannot afford to waste. To solve this problem one has to look back in the coding literature, to find two simple, yet efficient, methods to soft-decode block codes. The first one is due to Wolf [10] who showed that linear cyclic block codes could be soft-decoded using a trellis thus giving the possibility to utilize efficient algorithms like SOVA and BCJR. For example, a Hamming code can be thought of as a convolutional code of rate 1. Fig. 6 shows a section of the trellis of a (15, 11) Hamming code generated by this method.

The second one is due to Chase [11] who defined a class of algorithms working on the following idea. At high SNRs, it is very likely that the correct codeword C of a (n, k, d) code is located inside the sphere with radius $(d-1)$ around Y , where Y is simply the hard decoded version of the noisy received sequence RS . Hence, Chase algorithms, search for the

codewords located inside this sphere, and the closest codeword in Euclidean distance rather than Hamming distance is selected. Finally, the winning codeword is decoded using an algebraic decoder.

These two methods have led to the construction of two types of serially concatenated Turbo codes [14]. The first scheme is due to Hagenauer [12] and the second to Pyndiah [13] who designed the so-called Block Turbo Codes (BTC).

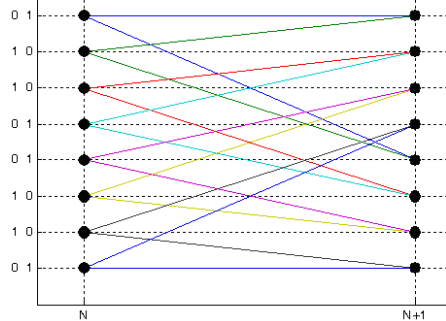


Figure 6. Trellis of a (15, 11) Hamming code

In our application, we decided to use Hagenauer’s method in combination with log-MAP SISO modules for the decoding. Fig. 7 shows the structure of our Turbo decoder. The performance of the system for various Hamming codes on the AWGN and Rayleigh channels using BPSK modulation is given in Fig. 8. It has been shown that some of these high rate codes perform only at 1.2dB from the Shannon limit [12].

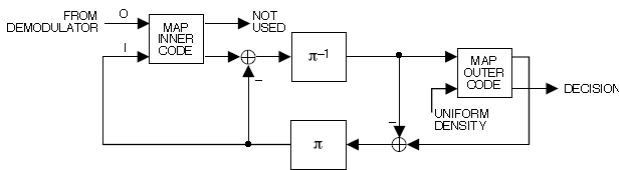


Figure 7. Turbo decoder for a serially concatenated Hamming code [14]

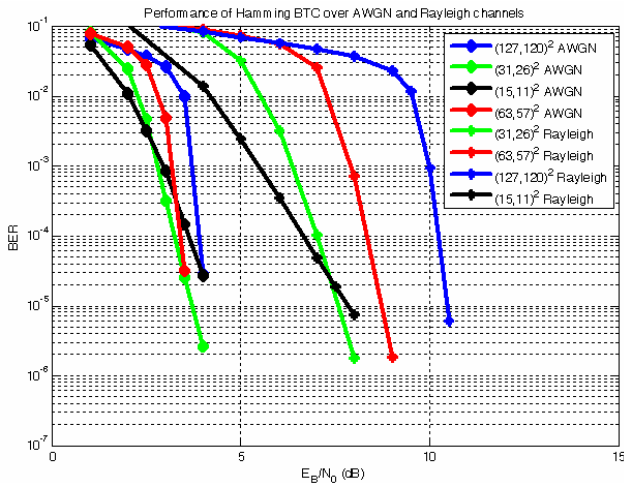


Figure 8. Performance of various Hamming BTCs after 4 iterations.

In our system, the different WT subbands do not have the same importance as far as visual rendering is concerned. This is the reason why we use an Unequal Error Protection (UEP) strategy to assign a $(31, 26)^2$ Hamming code to the most significant subbands (LL3) and a $(63, 57)^2$ Hamming code to the other subbands. This yields an overall code rate $R = 0.74$ which is much higher than the values found in the literature for this type of application.

The last step was to use the 16DAPSK modulation in conjunction with BTCs where a suitable bit metric had to be found for iterative decoding. For that purpose, we have chosen the APP bit metric proposed by Ishibashi et al. [15]. This metric is quite simple to implement and has also the advantage of not requiring any CSI. Fig. 9 shows a transmission of a WTSOM image using the above described techniques.



a) Received WTSOM image, no ECC, SNR=15dB, BER=4.4%, $f_D T_s = 0.001$, PSNR=19.04 dB
b) Received WTSOM image, after ECC, 2 Turbo iterations PSNR=25.57dB

Figure 9. WTSOM Turbo coded transmission example

The system described up to now can be used alone or in combination with a post-reception image restoration algorithm described in the next section.

IV. PDE BASED RESTORATION ALGORITHM

As image processing applications require higher levels of reliability and efficiency, mathematical image processing, especially PDE-based approaches, have become very popular over the last two decades. Let $I(x, y) = I$ be a still, gray-level image, represented by a function of $\Omega \subset \mathcal{R}^2 \rightarrow \mathcal{R}$ that associates to a pixel $(x, y) \in \Omega$ its gray-level value $I(x, y)$; Ω is the support of the image. In [16], Alvarez *et al.* show that Perona-Malik’s well known anisotropic diffusion model for edge-preserving filtering [17] can also be written as follows:

$$\begin{cases} \frac{\partial I(x, y, t)}{\partial t} = c_{\xi} I_{\xi\xi} + c_{\eta} I_{\eta\eta} \\ I(x, y, 0) = I_0(x, y) \end{cases} \quad (5)$$

where I_0 denotes a noisy version of I , $I_{\xi\xi}$ and $I_{\eta\eta}$ the second derivatives of I in orthogonal directions ξ and η , and η and ξ the gradient and orthogonal-gradient directions.

For $c_\xi = 1$ and $c_\eta = 1$, this equation actually is the heat equation, hence the concept of *diffusion*: each gray-level intensity $I(x, y)$ happens to diffuse over neighbouring pixels $(x \pm \partial x, y \pm \partial y)$ for a given time t , creating a (Gaussian) smoothing effect on the overall image. Knowing that unit vector ξ is actually tangential to the edge curve for every point of the image, as shown in Figure 10, we can easily understand how by describing a c_ξ -weighted (with $c_\eta = 0$), tangential diffusion of $I(x, y)$ along local edges, Alvarez *et al.*'s formulation can allow us to interpolate existing structures into missing areas.

In [18] a 2nd order digital inpainting model for error concealment in color JPEG images was proposed. This model is based on Tschumperlé's tensor-based diffusion model, and can be written as:

$$\begin{cases} \frac{\partial I_i}{\partial t} = \text{trace}(\mathbf{T}\mathbf{H}_i) + \lambda_e(I_i - I_0) & \text{for } i=1,2,\dots,m \\ I_i(x,y,0) = I_0(x,y) \end{cases} \quad (6)$$

where $\mathbf{I} = [I_1 \ I_2 \ \dots \ I_m]^T$ denotes a vector-valued function (e.g. a RGB image with $m = 3$), \mathbf{H}_i the Hessian matrix of I_i , $\lambda_e = \lambda(1 - \chi_D)$ an extended Lagrange multiplier using the characteristic function (mask) $\chi_D(x, y)$ of the inpainting domain D ($\chi_D = 1$ if inside, 0 if not), and where matrix \mathbf{T} is referred to as a *diffusion tensor*, and defines a direction and strength for the smoothing effect based on local geometry. More details about this inpainting model can be found in [18].

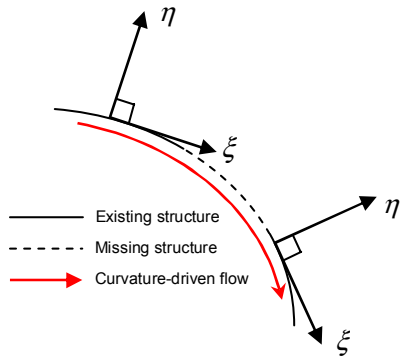


Figure 10. Interpolation using geometry-driven flows

In order to make use of the reconstruction algorithm described above one needs a way to build an error mask from the received image. Moreover, it is required not to add any more redundancy to the BTC coded image. The idea we follow is simply to use the reliability information at the output of the Turbo decoder. In fact, after a few iterations (2 iterations have shown to be enough) the reliability of the decoding is high enough to build a quite precise mask from a selected threshold.

Fig. 11 gives an example of such a mask where a white square represents a possible error position.



Figure 11. Error mask built from the output of the Turbo decoder

We then apply the following algorithm to the received image:

- First inpainting phase based on Tschumperlé's diffusion model is applied on all LL3 subbands,
- WT level LL2 is reconstructed using the inpainted LL3, the error mask $\chi_D(x, y)$ is up-sampled to match the LL2 size, the second inpainting phase is applied to LL2,
- Previous step is repeated up to the last level which represents the decoded and error-concealed image.

Fig. 12 shows an example of the reconstruction process applied on a received image.



a) Received WTSOM image, after ECC, 2 Turbo iterations, PSNR=25.57dB



b) Received WTSOM image, after inpainting phase PSNR=26.53dB

Figure 12. WTSOM transmission with reconstruction

Having described a two-step transmission strategy in the above, we present the behaviour of the WTSOM scheme when the Doppler frequency varies and draw some conclusions in the next section.

V. RESULTS AND CONCLUSIONS

To test the robustness of our scheme, we have performed transmissions over three decades of the normalized Doppler frequency $f_D T_S$ ($f_D =$ Doppler frequency in Herz and $T_S =$

symbol time in seconds). Fig. 13 summarizes the behaviour of the WTSOM scheme in terms of Peak Signal-to-Noise Ratio % (PSNR%) which represents the amount of PSNR in percentage lost during transmission. The values are averaged over 50 transmissions per $f_D T_s$ value. One can notice the relative insensitivity of the system to the Doppler frequency of the channel.

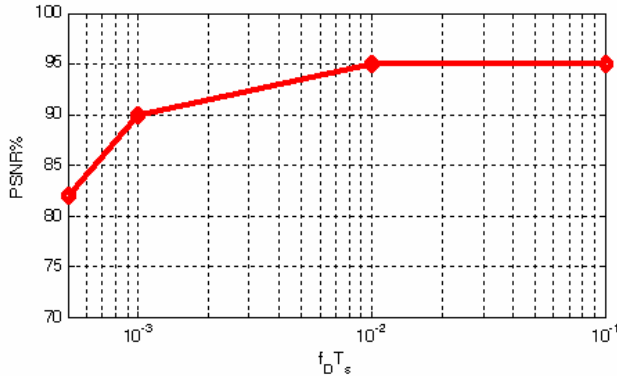


Figure 13. WTSOM PSNR% as a function of $f_D T_s$

In this paper we have presented a robust image transmission scheme suitable for frequency flat fading channels. The system yields very good visual quality even with BER as high as 4%, a value quite unusual in image transmission applications. Furthermore, this scheme only requires 26% redundancy (to be compared to the average value of 70% commonly found in similar applications) for ECC. The ECC step can be completed by an original PDE restoration algorithm to further increase the visual quality. This scheme is particularly well suited for low complexity image transmission applications in wireless ad-hoc sensor networks.

REFERENCES

- [1] F. Dufaux, F. Baruffa, G. Frescura, D. Nicholson, JPWL - an extension of JPEG 2000 for wireless imaging, IEEE ISCAS, Mai 2006.
- [2] V. Stankovic, R. Hamzaoui, and Z. Xiong, Fast forward error protection algorithms for transmission of packetized multimedia bitstreams over varying channels, in Proc. IEEE Int. Conf. Communication, Anchorage, AK, May 2003, pp. 40–44.
- [3] N. Thomos, N. Boulgouris, M. Strinzis, Optimized transmission of JPEG2000, streams over wireless channels, IEEE Transactions of image processing, Vol. 15, N°1, January 2006.
- [4] O. Aitsab, R. Pyndiah, B. Solaiman, "Joint optimization of multidimensional SOFM codebooks with QAM modulations for vector quantized image transmission", 3rd International workshop in signal/image processing, pp. 3-6, Manchester, UK, November 1996.
- [5] C. Chatellier, H. Boeglen, C. Perrine, C. Olivier, O Haeberlé, A robust joint source channel coding scheme for image transmission over the ionospheric channel, *ELSEVIER SPIC*, August 2007..
- [6] M. Paetzold, Mobile fading channels, Wiley, 2002.
- [7] COST 207, "Digital land mobile radio communications", Office for Official Publications of the European Communities, Final Report, Luxembourg, 1989.
- [8] Svensson, N.A.B. On differentially encoded star 16QAM with differential detection and diversity Vehicular Technology, IEEE Transactions on Volume 44, Issue 3, Aug. 1995 Page(s): 586-593.

- [9] H. Boeglen, C. Chatellier, O. Haeberle, "On the robustness of a joint source-channel coding scheme for image transmission over non frequency selective Rayleigh fading channels", ICTTA'06: 2nd IEEE International Conference on Information & Communication Technologies: From theory to applications, Damascus Syria, April 2006.
- [10] J. Wolf, Efficient maximum likelihood decoding of linear block codes using a trellis, Information Theory, IEEE Transactions on, Volume 24, Issue 1, Jan 1978 Page(s): 76 – 80
- [11] D. Chase. "A class of algorithms for decoding block codes with channel measurement information," IEEE Trans. on Information Theory, Vol.18, No.1, pp. 170–182, January 1972.
- [12] Hagenauer, J. Offer, E. Papke, L., Iterative decoding of binary block and convolutional codes, Information Theory, IEEE Transactions on, Volume 42, Issue 2, Mar 1996 Page(s): 429 – 445.
- [13] R. Pyndiah. "Near optimum decoding of product codes: block turbo codes" IEEE Trans. on communications, Vol. 46, No. 8, pp. 1003–1010, August 1998.
- [14] Sergio Benedetto, Dariush Divsalar, Guido Montorsi, and Fabrizio Pollara, "Serial concatenation of interleaved codes: Performance analysis, design and iterative decoding", JPL TDA Progress Report, vol. 42-126, Aug. 1996.
- [15] K. Ishibashi, H. Ochiai, and R. Kohno, "Low Complexity Bit-Interleaved Coded DAPSK for Rayleigh Fading Channels", *IEEE Journal on Selected Areas - Issue on Differential and Noncoherent Wireless Communications*, vol. 23, no. 9, Sept. 2005.
- [16] L. Alvarez, P-L. Lions, J-M. Morel, "Image selective smoothing and edge detection by nonlinear diffusion II", *SIAM Journal on Numerical Analysis* 29 (3), pp. 845-866, 1992.
- [17]] P. Perona, J. Malik, "Scale-space and edge detection using anisotropic diffusion", *IEEE transactions on Pattern Analysis and Machine Intelligence* 12 (7), pp. 629-639, 1990.
- [18] P. Bourdon, C. Chatellier, B. Augereau, and C. Olivier, "A multi-resolution, geometry-driven error concealment method for corrupted JPEG color images", *EURASIP Signal processing: Image Communication* 20 (7), pp. 681-694, August 2005.